

16-Element Superconducting Nanowire Single-Photon Detector for Gigahertz Counting at 1550-nm

Timothy M. Rambo,^{1, a)} Amy. R. Conover,¹ and Aaron J. Miller¹
Quantum Opus LLC. Novi, Mi

(Dated: 29 March 2021)

We present a linearly arrayed, 16-element, superconducting nanowire single-photon detector with 83.4% system detection efficiency at 1550 nm and a mean per-element dead-time of 9.6-ns —enabling counting at 1 giga-count per second with > 50% System Detection Efficiency. This device was designed and fabricated in an existing scalable commercial process.

I. INTRODUCTION

Superconducting nanowire single-photon detectors (SNSPDs) have proliferated the optics community in recent years due to their unique combination of high detection efficiency ($\geq 98\%$)¹, extremely low dark counts ($< 1/s$ for UV², $< 100/s$ commercially available at 1550 nm), broad spectral response from UV to mid-infrared²⁻⁴, precise timing accuracy (< 4.3 ps FWHM intrinsic timing jitter at 1550 nm for NbN nanowires, and < 10.6 ps FWHM intrinsic timing jitter at 1550 nm for MoSi)^{5,6}, and recent discovery of true photon number resolving capacity^{7,8}. Diverse fields as quantum optics⁹⁻¹², spectroscopy¹³, and free-space optical communications^{14,15} have leveraged SNSPDs with great success and driven the rise of commercially available SNSPD systems. Commercial SNSPDs are typically single-element devices which can achieve count rates ~ 10 MHz and have small active areas designed for coupling to single-mode fibers. To keep up with the evolving demands of the research community, SNSPD technology must increase its achievable count-rates and active areas. While it is possible to change the electrical characteristics by adding series resistance to achieve higher count rates^{16,17} and increase the footprint of SNSPDs¹, meandering the wires over a larger area increases the kinetic inductance which slows recovery time. One approach to circumvent this counteraction is to produce multi-element SNSPDs, where the device is fabricated to cover a larger area but split into many active areas instrumented either independently¹⁸ or jointly^{19,20}. Recent work has also shown the viability of detectors made of out micron-scale superconducting wires with thinner superconducting films²¹. Here, we present a linearly-arrayed, 16-element, SNSPD which achieves 83.4% system detection efficiency (SDE) and is capable of counting with $\geq 50\%$ at ~ 1 GHz countrate. This device was developed in a commercial process for immediately scalable production.

II. FABRICATION

Our device was fabricated on a Silicon substrate topped with a ~ 100 -nm thick thermal oxide layer beneath a gold

mirror. An additional oxide layer separated the device and the mirror, creating the back-short for a $\lambda/4$ optical cavity formed around the device. The SNSPD itself was fabricated by depositing a 7 nm thick proprietary metal and amorphous silicide film, with a 5 K critical temperature on top of the back-short. We lithographically patterned this film into a meandered wire geometry with 60 nm wire-width and 50% fill factor to create 16 linearly arrayed, individually wired, $16 \mu\text{m} \times 1 \mu\text{m}$, sub-elements to create the SNSPD device. The top side of the $\lambda/4$ cavity was created using a two-layer dielectric coating to enhance absorption at 1550 nm. As a final step to the fabrication process, the wafer was deep etched to create a keyhole like chip for the detector compatible with the self-alignment technique²². An optical micrograph of the device chip and an up-close view of the linearly arrayed, independently wired, elements is shown in Figure 1.

III. CHARACTERIZATION

The device was characterized at a temperature of 2.3K in an Opus One rack-mountable Gifford-McMahon cryostat with illumination at 1550 nm provided via self-alignment to OFS #36484 four-mode graded index fiber (FMF). The detector was electrically instrumented using a patent pending, dc-coupling, anti-latch circuit²³ —which requires a single-coax line per element as opposed to the two lines required for a typical cryogenic bias tee—and the commercially available Quantum Opus SNSPD Bias and Amplification Module, a self-contained 1U system. To characterize SDE, a tunable continuous wave laser was injected into the FMF from single-mode fiber (SMF) via a series of cascaded attenuators. Incident photon flux was set to $\sim 3 \times 10^6/s$ for the measurement of SDE as a function of device bias for each element. Net SDE across all elements was 83.4% with 71,000 dark counts per second. FMF laser sources are not readily available, but there has been an exploration²⁴ of how the higher order modes in the fiber couple to an SNSPD with similar total footprint to this one, and how the increased fiber core size affects dark rates compared to SMF coupling.

Black body radiation is the dominant source of noise in this experiment. The flux of black body photons at room temperature tends to become significant for wavelengths > 1700 nm which are very poorly guided by SMF, typically creating 100 dark counts per second on commercially available SNSPDs optimized for 1550nm. However, the FMF in this experiment

^{a)}Electronic mail: tim@quantumopus.com.

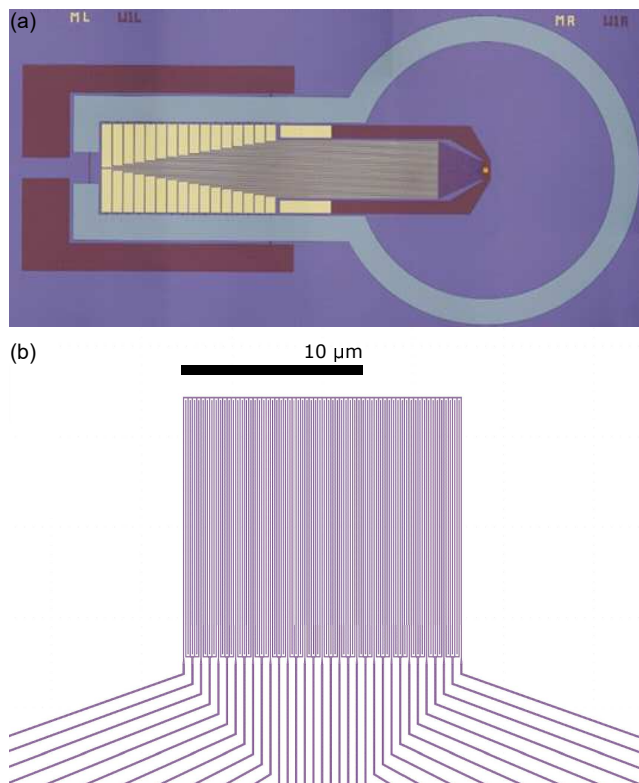


FIG. 1. (a) An optical micrograph showing the structure of the multi-element SNSPD chip. The round region at the end is 2.5mm in diameter for compatibility with zirconia sleeves for self-alignment to fiber and the SNSPD is too small to see. (b) Zoomed in view of the multi-element detector. This is a negative image, white shows the presence of superconductor and purple the absence.

supports multiple modes at wavelengths even beyond 2 μm resulting in an elevated dark rate which would not be present in all applications or for all fiber types. The dark counts are further enhanced by the fact that the elements in this device have a relatively long plateau of saturated 1550-nm detection efficiency as a function of bias currents. A long plateau is suggestive of a better response for the blackbody photons than for devices which barely reach saturation. Figure 2 shows a system detection efficiency and dark count rate versus bias plot for one of the elements. Charting the efficiency as a function of element number shows that the peak photon absorption occurs off center of the sub-element array. This is due to alignment uncertainty in the fabrication process and fiber tolerances which cause an offset between the center of the key-hole structure and the SNSPD.

To measure reset-time to full efficiency, we swept incident photon rates through the range of $\sim 10^3/\text{s}$ to $\sim 10^8/\text{s}$ with the SNSPDs biased to the current which gives 5,000 dark counts per second. The resulting counts versus attenuation data was then fit using a Poisson model to determine the reset-time. Figure 3 shows data and the Poisson modelling for a single element as well as a summary of data for all elements. Measurements across all sub-elements of the SNSPD yielded an average reset-time to full efficiency of 9.6 ns with 2.2 ns stan-

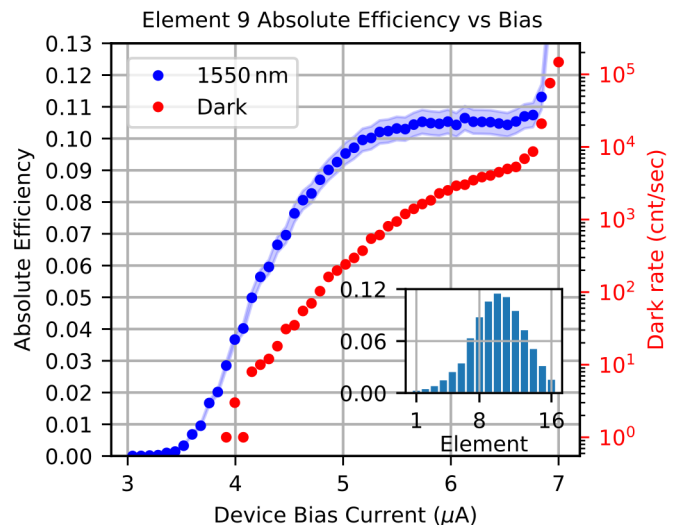


FIG. 2. Absolute efficiency and dark counts for element 9 of the SNSPD as a function of bias current. (inset) Efficiency at the bias current which yields 5,000 dark for each element.

dard deviation, corresponding to an average maximum full-efficiency pulsed count rate of 107.6 MHz. Using these numbers, we calculate efficiency as a function of incident photon rate for the entire device, and this shows the device is capable of counting at $\geq 50\%$ SDE with ~ 1 GHz incident photon rate under uniform illumination.

Jitter was measured using a 1550-nm, mode-locked fiber laser (Nuphoton EDFL-PICO-1560-5-50-FCA) and a Swabian Time Tagger Ultra. Each element was biased to a current which corresponded to 5,000 dark counts per second for the jitter measurement. Jitter was measured as a correlation between the laser electrical reference and the electrical pulse output from each SNSPD element. Systemic sources of jitter were the intrinsic jitter of the Time Tagger Ultra, $J_{TT} = 22$ ps FWHM, and the optical pulse width of the laser, $J_{pulse} = 8$ ps FWHM. Jitter contribution from the electrical reference was determined to be negligible compared to the other sources. The FWHM jitter contribution of the SNSPD, J_{SNSPD} , was extracted from the measured FWHM jitter, J_{meas} , using the following relation:

$$J_{meas}^2 = J_{SNSPD}^2 + J_{TT}^2 + J_{pulse}^2. \quad (1)$$

A typical timing response histogram can be seen in Figure 1. Mean jitter across all elements was 86.1 ps with a standard deviation of 10.2 ps.

One element had significantly worse jitter than the others. It also had a reduced switching current, no detection efficiency plateau, and reduced count-rate compared to the other elements. This suggests a constriction or defect in this one element. In a standard, single-element, SNSPD design this defect would have limited the performance of an entire device, but here affects the performance of only 1/16th of the device.

Element-to-element crosstalk was measured pair-wise in all possible combinations. This was done by biasing a given pair

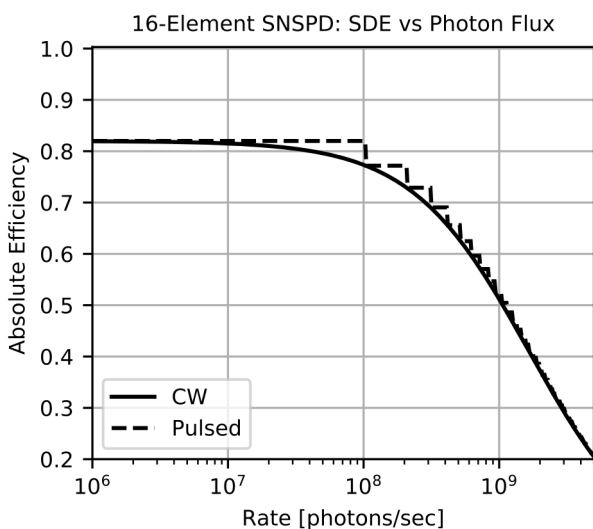
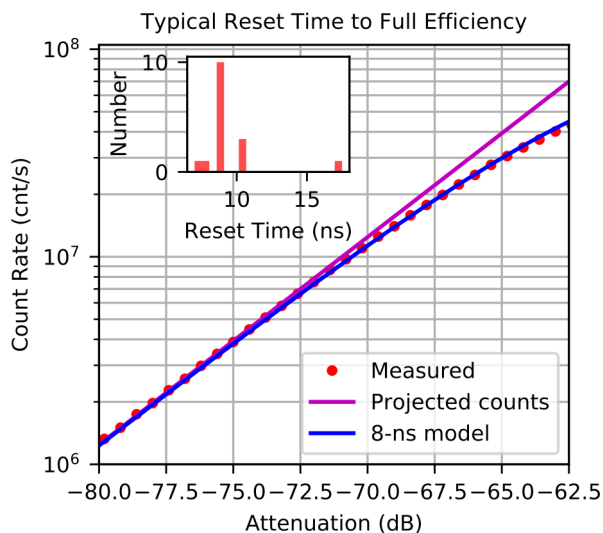


FIG. 3. (top) Count-rate versus source attenuation measurement for SNSPD element 12. Modeled versus projected counts show 8-ns reset time. Inset shows histogram of reset times across all elements. Histogram of full-efficiency reset times of the sub-elements in the detector and calculated net detection efficiency versus incident photon flux from a CW source. (bottom) Model of SDE versus incident photon flux based on measured reset times of elements assuming uniform illumination. SDE is $\geq 50\%$ for count rates up to 1 GHz.

of elements E_i and E_j to the 5,000 dark count bias, then biasing E_i into a high dark count regime $\sim 10^6$ dark counts/s and measuring the increase in counts on E_j as a percent of the total count rate on E_i . The maximum observed increase in counts for any E_j was 5% of the counts on E_i , with most i, j combinations yielding $\ll 1\%$ increase. When repeated with starting bias currents which corresponded to 500 dark counts per second on each channel, the maximum extra counts observed on any E_i was 0.1% with the majority of i, j combinations giving $\ll 0.02\%$, nearly an order of magnitude improvement. Because the cross-talk of a handful of element pairs dominates

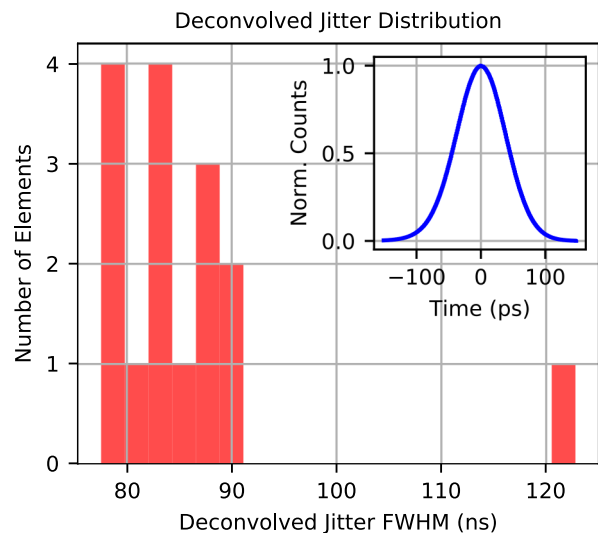


FIG. 4. (Distribution of deconvolved jitters across all elements. Inset shows a timing distribution from a single element.

the others, bias adjustment would only be necessary on a subset of elements to suppress the effect. This would help to mitigate the efficiency penalty of lowering bias currents. A full plot of the results from both bias regimes can be seen in Figure 5. Using channel E_i as the start channel on a time-tagger, we observed that the crosstalk counts on stop channel E_j were delayed by ~ 1 ns. This suggests that it may also be possible to remove or reduce the cross-talk using temporal gating.

IV. CONCLUSION

We presented an FMF coupled 16-element SNSPD created from an existing, immediately scalable, commercial process. This multi-element device showed 83.4% net system detection efficiency with 71,000 dark counts per second, average per-pixel timing jitter of 86.1 ps FWHM, and average per-pixel reset time of 9.675 ns—meaning the device can count with $> 50\%$ system detection efficiency at 1GHz mean photon rate. Dark counts are elevated above standard commercial SNSPDs due to the FMF-coupling, these could be drastically reduced by coupling the device to SMF (which achieves dark count rates of < 100 /s on standard commercial devices) or by using cold filtering techniques²⁵. We expect that increasing availability of this type of high-count rate, high efficiency, SNSPD will drive new applications in many fields.

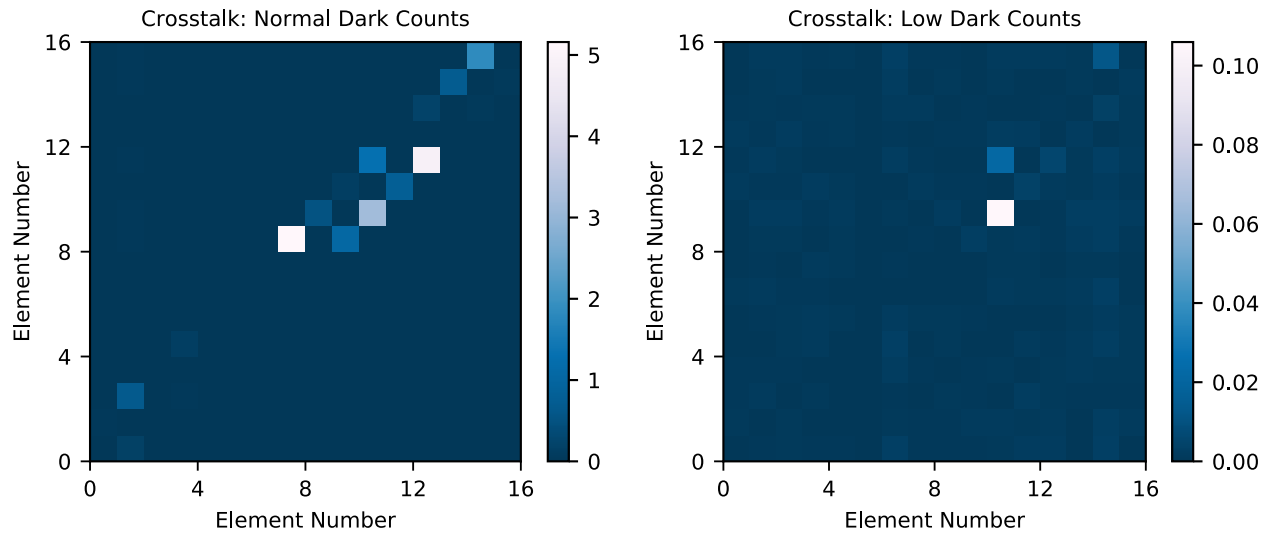


FIG. 5. (left) Crosstalk percent for each element pair when one channel is biased to 5,000 dark counts per second and the other to 100,000 dark counts per second. (right) Crosstalk percent for each element pair when one channel is biased to 500 dark counts per second and the other to 100,000 dark counts per second

ACKNOWLEDGMENTS

We wish to acknowledge the support of NASA grant 80NSSC19C0141 for helping to make this research possible.

¹D. V. Reddy, A. E. Lita, S. W. Nam, R. P. Mirin, and V. B. Verma, “Achieving 98% system efficiency at 1550 nm in superconducting nanowire single photon detectors,” in *Rochester Conference on Coherence and Quantum Optics (CQO-11)* (Optical Society of America, 2019) p. W2B.2.

²E. E. Wollman, V. B. Verma, A. D. Beyer, R. M. Briggs, B. Korzh, J. P. Allmaras, F. Marsili, A. E. Lita, R. P. Mirin, S. W. Nam, and M. D. Shaw, “Uv superconducting nanowire single-photon detectors with high efficiency, low noise, and 4 k operating temperature,” *Opt. Express* **25**, 26792–26801 (2017).

³L. Chen, D. Schwarzer, J. A. Lau, V. B. Verma, M. J. Stevens, F. Marsili, R. P. Mirin, S. W. Nam, and A. M. Wodtke, “Ultra-sensitive mid-infrared emission spectrometer with sub-ns temporal resolution,” *Opt. Express* **26**, 14859–14868 (2018).

⁴G. G. Taylor, D. Morozov, N. R. Gemmill, K. Erotokritou, S. Miki, H. Terai, and R. H. Hadfield, “Photon counting lidar at 2.3 μ m wavelength with superconducting nanowires,” *Opt. Express* **27**, 38147–38158 (2019).

⁵B. Korzh, Q.-Y. Zhao, S. Allmaras, Jason P. and Frasca, T. M. Autry, E. A. Bersin, A. D. Beyer, R. M. Briggs, B. Bumble, M. Colangelo, G. M. Crouch, A. E. Dane, T. Gerrits, A. E. Lita, F. Marsili, G. Moody, C. Peña, E. Ramirez, J. D. Rezac, N. Sinclair, M. J. Stevens, A. E. Velasco, V. B. Verma, E. E. Wollman, S. Xie, D. Zhu, P. D. Hale, M. Spiropulu, K. L. Silverman, R. P. Mirin, S. W. Nam, A. G. Kozorezov, M. D. Shaw, and K. K. Berggren, “Demonstration of sub-3 ps temporal resolution with a superconducting nanowire single-photon detector,” *Nature Photonics* **14**, 250–255 (2020).

⁶M. Caloz, B. Korzh, E. Ramirez, C. Schönenberger, R. J. Warburton, H. Zbinden, M. D. Shaw, and F. Bussi eres, “Intrinsically-limited timing jitter in molybdenum silicid superconducting nanowire single-photon detectors,” *Journal of Applied Physics* **126**, 164501 (2019), <https://doi.org/10.1063/1.5113748>.

⁷C. Cahall, K. L. Nicolich, N. T. Islam, G. P. Lafyatis, A. J. Miller, D. J. Gauthier, and J. Kim, “Multi-photon detection using a conventional superconducting nanowire single-photon detector,” *Optica* **4**, 1534–1535 (2017).

⁸D. Zhu, M. Colangelo, C. Chen, B. A. Korzh, F. N. C. Wong, M. D. Shaw, and K. K. Berggren, “Resolving photon numbers using a superconducting nanowire with impedance-matching taper,” *Nano Letters* **20**, 3858–3863 (2020), pMID: 32271591, <https://doi.org/10.1021/acs.nanolett.0c00985>.

⁹S. Agne, T. Kauten, J. Jin, E. Meyer-Scott, J. Z. Salvail, D. R. Hamel, K. J. Resch, G. Weihs, and T. Jennewein, “Observation of genuine three-photon interference,” *Phys. Rev. Lett.* **118**, 153602 (2017).

¹⁰H. Wang, J. Qin, X. Ding, M.-C. Chen, S. Chen, X. You, Y.-M. He, X. Jiang, L. You, Z. Wang, C. Schneider, J. J. Renema, S. H ofling, C.-Y. Lu, and J.-W. Pan, “Boson sampling with 20 input photons and a 60-mode interferometer in a 10^{14} -dimensional hilbert space,” *Phys. Rev. Lett.* **123**, 250503 (2019).

¹¹U. Paudel, J. J. Wong, M. Goggin, P. G. Kwiat, A. S. Bracker, M. Yakes, D. Gammon, and D. G. Steel, “Direct excitation of a single quantum dot with cavity-spdc photons,” *Opt. Express* **27**, 16308–16319 (2019).

¹²N. T. Islam, C. C. W. Lim, C. Cahall, J. Kim, and D. J. Gauthier, “Provably secure and high-rate quantum key distribution with time-bin qudits,” *Science Advances* **3** (2017), 10.1126/sciadv.1701491, <https://advances.sciencemag.org/content/3/11/e1701491.full.pdf>.

¹³T. L. Atallah, A. V. Sica, A. J. Shin, H. C. Friedman, Y. K. Kahrobai, and J. R. Caram, “Decay-associated fourier spectroscopy: Visible to shortwave infrared time-resolved photoluminescence spectra,” *The Journal of Physical Chemistry A* **123**, 6792–6798 (2019).

¹⁴D. M. Boroson, B. S. Robinson, D. V. Murphy, D. A. Buri- anek, F. Khatri, J. M. Kovalik, Z. Sodnik, and D. M. Cornwell, “Overview and results of the Lunar Laser Communication Demonstration,” in *Free-Space Laser Communication and Atmospheric Propagation XXVI*, Vol. 8971, edited by H. Hemmati and D. M. Boroson, International Society for Optics and Photonics (SPIE, 2014) pp. 213 – 223.

¹⁵B. E. Vyhnalek, S. A. Tedder, and J. M. Nappier, “Performance and characterization of a modular superconducting nanowire single photon detector system for space-to-Earth optical communications links,” in *Free-Space Laser Communication and Atmospheric Propagation XXX*, Vol. 10524, edited by H. Hemmati and D. M. Boroson, International Society for Optics and Photonics (SPIE, 2018) pp. 369 – 377.

¹⁶J. K. W. Yang, A. J. Kerman, E. A. Dauler, V. Anant, K. M. Rosfjord, and K. K. Berggren, “Modeling the electrical and thermal response of superconducting nanowire single-photon detectors,” *IEEE Transactions on Applied Superconductivity* **17**, 581–585 (2007).

- ¹⁷T. M. Rambo, A. R. Conover, and A. J. Miller, “Two Billion Photon Per Second, One Photon at a Time,” in *Single-Photon Workshop 2019 Book of Abstracts*, edited by H. Hemmati and D. M. Boroson (2019) p. 165.
- ¹⁸J. Huang, W. Zhang, L. You, C. Zhang, C. Lv, Y. Wang, X. Liu, H. Li, and Z. Wang, “High speed superconducting nanowire single-photon detector with nine interleaved nanowires,” *Superconductor Science and Technology* **31**, 074001 (2018).
- ¹⁹E. E. Wollman, V. B. Verma, A. E. Lita, W. H. Farr, M. D. Shaw, R. P. Mirin, and S. W. Nam, “Kilopixel array of superconducting nanowire single-photon detectors,” *Opt. Express* **27**, 35279–35289 (2019).
- ²⁰J. P. Allmaras, E. E. Wollman, A. D. Beyer, R. M. Briggs, B. A. Korzh, B. Bumble, and M. D. Shaw, “Demonstration of a thermally coupled row-column snspd imaging array,” *Nano Letters* **20**, 2163–2168 (2020), pMID: 32091221, <https://doi.org/10.1021/acs.nanolett.0c00246>.
- ²¹J. Chiles, S. M. Buckley, A. Lita, V. B. Verma, J. Allmaras, B. Korzh, M. D. Shaw, J. M. Shainline, R. P. Mirin, and S. W. Nam, “Superconducting microwire detectors based on wsi with single-photon sensitivity in the near-infrared,” *Applied Physics Letters* **116**, 242602 (2020), <https://doi.org/10.1063/5.0006221>.
- ²²A. J. Miller, A. E. Lita, B. Calkins, I. Vayshenker, S. M. Gruber, and S. W. Nam, “Compact cryogenic self-aligning fiber-to-detector coupling with losses below one percent,” *Opt. Express* **19**, 9102–9110 (2011).
- ²³T. M. Rambo and A. J. Miller, U.S. Patent App. No. 16/399,207 (2019).
- ²⁴B. E. Vyhnalek, S. A. Tedder, E. J. Katz, and J. M. Nappier, “Few-mode fiber coupled superconducting nanowire single-photon detectors for photon efficient optical communications,” in *Free-Space Laser Communications XXXI*, Vol. 10910, edited by H. Hemmati and D. M. Boroson, International Society for Optics and Photonics (SPIE, 2019) pp. 62 – 75.
- ²⁵C. Zhang, W. Zhang, L. You, J. Huang, H. Li, X. Sun, H. Wang, C. Lv, H. Zhou, X. Liu, Z. Wang, and X. Xie, “Suppressing dark counts of multimode-fiber-coupled superconducting nanowire single-photon detector,” *IEEE Photonics Journal* **11**, 1–8 (2019).
- ²⁶D. V. Reddy, A. E. Lita, S. W. Nam, R. P. Mirin, and V. B. Verma, “Achieving 98% system efficiency at 1550 nm in superconducting nanowire single photon detectors,” in *Rochester Conference on Coherence and Quantum Optics (CQO-11)* (Optical Society of America, 2019) p. W2B.2.